Eurasian Journal of Physics and Functional Materials

2026, 10(3), 260-268

Features of the structure, dielectric and conductive properties of polycrystals $Na_3Fe_2(PO_4)_3$ and $Na_3FeTi(PO_4)_3$

A.A. Nogai[1], E.A. Nogai[1], D.D. Aikimbayeva[1], A.S. Nogai[1], G.G. Tatkeeva[1*], N.F. Zikrillaev[2], A.B. Utegulov[1], O.N. Leznaya[1], V.A. Dyakov[1]

[1]Energy Institute of the Saken Seifullin Kazakh Agrotechnical University, Astana, Kazakhstan

[2]Islam Karimov Tashkent State Technical University, Tashkent, Uzbekistan

E-mail: nogay06@mail.ru

DOI: **10.32523/ejpfm.2026100305**
Received: 08.08.2026 - after revision

This article presents the results of a study into the structure, dielectric and conductive properties of $Na_3Fe_2(PO_4)_3$ and $Na_3FeTi(PO_4)_3$, obtained by the melt synthesis method. It has been established that $Na_3FeTi(PO_4)_3$ forms in the β-phase with hexagonal symmetry (sp. gr. $P\bar{3}c$), in contrast to α - $Na_3Fe_2(PO_4)_3$, which possesses a rhombohedral monoclinic distorted structure. Consequently, β - $Na_3FeTi(PO_4)_3$ is an ionic conductor and is capable of being easily polarised and exhibiting ionic conductivity. In contrast, α - $Na_3Fe_2(PO_4)_3$ exhibits dielectric properties, as the majority of the cation sublattice is dipole-ordered, whilst the remainder is structurally ordered. The fact that β - $Na_3FeTi(PO_4)_3$ polycrystals have higher conductivity at room temperature than α - $Na_3Fe_2(PO_4)_3$ suggests that they may be more promising for use as a cathode material.

Keywords: melt synthesis; polycrystals; structure; dielectric and conductive properties; sodium cations

Introduction

The growing demand for lithium-ion batteries (LIB) requires the search for alternative low-cost construction materials to develop competitive metal-ion

batteries [1–3]. Sodium-ion batteries (SIB) are an alternative to LIBs, as sodium-containing materials are significantly less expensive than lithium-containing ones [4–6]. However, due to the low energy parameters of SIB, it is necessary to improve their energy-efficiency indicators by searching for effective structural cathode materials. Among other types of cathode materials, orthophosphates from the NASICON family can be distinguished, as these substances can provide high conductivity and structural stability during multiple charge and discharge cycles in batteries. The development of new, inexpensive materials with a NASICON-type structure and higher ionic conductivity is necessary for the development of SIBs. Therefore, interest in materials from the NASICON family, as well as in technologies capable of enhancing their conductive properties, is growing. For example, melt-based methods for synthesizing $Na_3Fe_2(PO_4)_3$ polycrystals have significantly improved the conductive and capacitive properties of this orthophosphate for use as cathode materials in NIA [7–9].

Polycrystals of $Na_3FeTi(PO_4)_3$ also attract attention, since the following compositions have already been discovered from the NASICON structural family: $A_2FeTi(PO_4)_3$ ($A = Na, Rb$), $Na_2TiM(PO_4)$, which have rhombohedral framework crystal structures and high electrical capacitance properties [10, 11]. Therefore, the synthesis of $Na_3FeTi(PO_4)_3$ polycrystal by the melt-quenching method and the study of its structure, dielectric, and conductive properties are of interest. To identify the distinctive features of the dielectric and conductive properties of $Na_3FeTi(PO_4)_3$ polycrystal, it is advisable to compare its structure and properties with those of $Na_3Fe_2(PO_4)_3$ polycrystal, which is spontaneously polarized in the α-phase and an ionic conductor in the β-phase [12]. The properties of $Na_3FeTi(PO_4)_3$ and $Na_3Fe_2(PO_4)_3$ polycrystals are easy to interpret, since they have similar crystal frameworks and belong to the NASICON rhombohedral structural type. Their crystal structures are based on mixed octahedral–tetrahedral crystal frameworks $\{[FeTi(PO_4)_3]^{3-}\}_{3\infty}$, respectively. The resulting small M(1) and large M(2) cavities of the anionic crystal frameworks accommodate Na^+ cations, which can move from one cavity to another, creating conduction channels for mobile sodium cations [10, 12]. Information on the construction features of NASICON rhombohedral structural type samples is presented in [13, 14].

This study aims to investigate the structural characteristics and the dielectric and conductive properties of $Na_3FeTi(PO_4)_3$ and $Na_3Fe_2(PO_4)_3$ samples produced by the melt-synthesis method, with a view to selecting a more effective cathode.

Materials and methods

$Na_3FeTi(PO_4)_3$ and $Na_3Fe_2(PO_4)_3$ samples were prepared using the following reagents: Na_2CO_3, Fe_2O_3, TiO_2, and $NH_4H_2PO_4$ (all high-purity grades).

Polycrystals of $Na_3FeTi(PO_4)_3$ and $Na_3Fe_2(PO_4)_3$ were obtained by melt-quenching synthesis.

Structural studies of the samples were conducted using a D-8 diffractometer (CuKα radiation).

The dependences of the permittivity $\varepsilon(T,\omega)$ of the samples were measured in the temperature range $T = 300-450$ K and frequencies $\nu = 2$ kHz–1 MHz using an E7-30 immittance meter.

The permittivity (ε) was determined using the following formula:

$$\varepsilon = \frac{d}{S}\frac{1}{2\pi f Z \sin\varphi} \tag{1}$$

where d is the sample thickness; S is the electrode area on the sample surface; f is the linear frequency; Z is the sample's complex impedance; and φ is the phase shift angle.

The ionic conductivity of the samples was determined by the impedance method using VM-507 and VM-538 devices in the temperature range $T = 300-450$ K.

The complex impedance Z^* of the sample is measured by an impedance meter, and the modulus of the real part Z^* of the crystallite is determined by the dependence:

$$Z^* = Z' + jZ'' \tag{2}$$

The specific conductivity of the crystallite, σ_{cr}, of the samples was determined using the following formula:

$$\sigma_{cr} = \frac{d}{S}\frac{1}{Z^*_{cr}\cos\varphi} \tag{3}$$

where σ_{cr} is the specific conductivity of the grain; Z^*_{cr} is the complex resistance of the grain; d is the thickness of the sample (cm); S is the area (cm^2); φ is the phase shift angle.

From the temperature dependence of the conductivity, the activation energies of the charge carriers were determined using the following formula:

$$\Delta E = \frac{k\Delta \lg\sigma}{\Delta\left(\frac{1}{T}\right)}; \tag{4}$$

where ΔE is the charge carrier activation energy; k is the Boltzmann constant; σ is the grain conductivity; T is the temperature.

Results of the study and their discussion

To conduct the studies, it was necessary to synthesize polycrystals of $Na_3FeTi(PO_4)_3$ and $Na_3Fe_2(PO_4)_3$. These polycrystals were synthesized using the melt-quenching method due to its efficiency [8, 9].

After preparing the batch and mechanically processing them, they were pre-annealed for 2 hours at 350 °C. After repeated mechanical processing, the powders were pressed into tablets. The tablets were then placed in a heated furnace until a melt was formed, after which the melt droplets were rapidly cooled in a quenching device. The resulting precursors were then mechanically processed

and fired in a muffle furnace. The sample preparation process conditions are listed in Table 1.

Table 1.
Synthesis conditions for polycrystalline $Na_3FeTi(PO_4)_3$ and $Na_3Fe_2(PO_4)_3$ samples.

Samples	$Na_3FeTi(PO_4)_3$			$Na_3Fe_2(PO_4)_3$		
Synthesis Modes	Melting	Melt-quenching	Firing	Melting	Melt-quenching	Firing
Firing Temperature T, °C	1450	30	820	980	30	800
Melting Time, s	55	60		50	60	
Firing Time t, h			2			2
Cooling Time t, h to $T = 25$°C		0.011			0.011	
Temperature Cooling Rate $v = T/t$, °C/h		129545			86 818	

The synthesis resulted in dark-brown $Na_3Fe_2(PO_4)_3$ polycrystals, while gray $Na_3FeTi(PO_4)_3$ polycrystals were obtained. Both samples were tablet-shaped (10 mm in diameter and 1 mm thick).

The X-ray diffraction patterns of $Na_3Fe_2(PO_4)_3$ (1) and $Na_3FeTi(PO_4)_3$ (2) polycrystals, shown in Figure 1, show that both samples are characterized by clearly defined peaks.

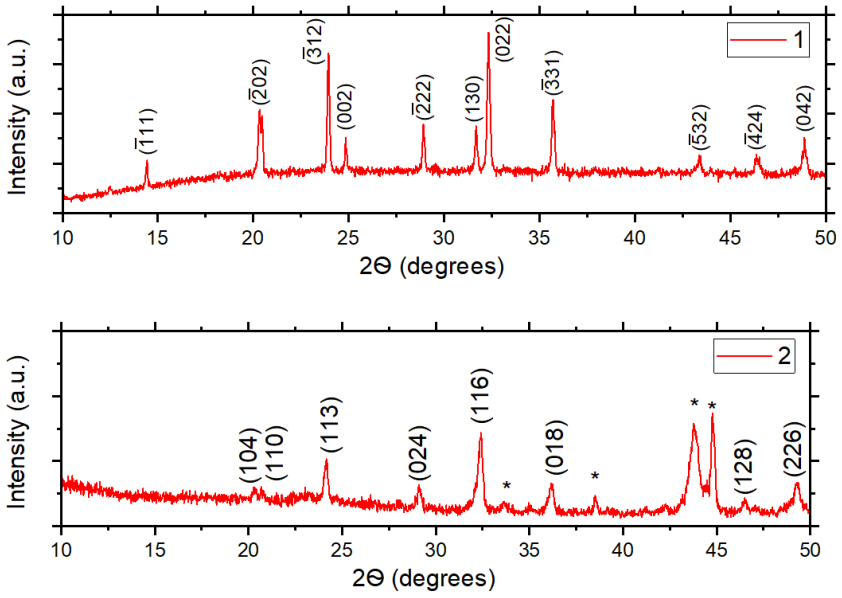

Figure 1. Diffraction patterns for polycrystals: 1 – $Na_3Fe_2(PO_4)_3$ and 2 – $Na_3FeTi(PO_4)_3$.

The structural parameters of $Na_3Fe_2(PO_4)_3$ samples were investigated in [8]; therefore, Table 2 presents the previously calculated structural data.

The analysis of diffractograms of $Na_3FeTi(PO_4)_3$ samples using the SellRef programme enabled the determination of structure parameters (see Table 2). It was found that $Na_3FeTi(PO_4)_3$ polycrystals have hexagonal symmetry (space group R-3c), just like $Na_2FeTi(PO_4)_3$, whose structure was studied in [10], as

many of the peaks in the diffraction patterns of these samples coincide. It has been established that the main reflections in the diffractogram of this sample are identified with high accuracy based on a hexagonal unit cell with $a = 8.602(6)$ Å, $c = 21.718(8)$ Å, and a space group of R-3c (the average difference between the measured and calculated values of the 2θ angles does not exceed 0.01°). The diffraction pattern also contains reflections from an as yet unidentified impurity phase (see Figure 1). The parameters found are in good agreement with those given in [10] for the $Na_2FeTi(PO_4)_3$ phase – $a = 8.6015(1)$ Å, $c = 21.718(1)$ Å, space group: R-3c. The presence of an impurity phase in the $Na_3FeTi(PO_4)_3$ samples is probably because their structural unit contains 3 Na atoms rather than 2.

Table 2.
Unit cell parameters of $Na_3FeTi(PO_4)_3$ and $Na_3Fe_2(PO_4)_3$ polycrystals.

Polycrystals	Sp.	Parameters of elementary cells						
Sample compositions	gr.	a, Å	b, Å	c, Å	α^0	β^0	γ^0	V, Å^3
$Na_3FeTi(PO_4)_3$	$R\bar{3}c$	8.602(6)		21.718(8)				1391.67
$Na_3Fe_2(PO_4)_3$	$C2/m$	15.1444	8.6840	21.5768		90.30		2837.65

When studying $Na_3FeTi(PO_4)_3$ and $Na_3Fe_2(PO_4)_3$ polycrystals, it is important to study the dielectric and ion-conducting properties of the low-temperature phases, since electrochemical processes occur at room temperature when they are used as cathode materials in SIB. Since α-$Na_3Fe_2(PO_4)_3$ is an AFE, it is appropriate to compare its dielectric properties with the properties of $Na_3FeTi(PO_4)_3$. Information on the dielectric properties of polycrystals makes it possible to obtain information on the ordering of the cationic sublattice of the crystalline framework, which must be used when analyzing the conductivity of the sample.

Figure 2 shows the dependences ($\varepsilon(T,\omega)$) of $Na_3Fe_2(PO_4)_3$ and $Na_3FeTi(PO_4)_3$ polycrystals, which demonstrate the dispersion of the permittivity parameters ε on frequency and temperature. For $Na_3Fe_2(PO_4)_3$ polycrystals, the polar α- and ion-conducting β-phases are clearly distinguished.

In α-$Na_3Fe_2(PO_4)_3$ polycrystals, polarization is associated with spontaneous polarization of the ASE type (P_s), i.e. with the displacement of sodium cations located in large M(2) cavities relative to the anionic crystal framework [12].

A sharp increase in the ε values of β-$Na_3Fe_2(PO_4)_3$ (upon transition to the β-phase) is associated with an increase in the symmetry of the structure, leading to dipole disordering of the cationic sublattice.

An increase in the slope of the $\varepsilon(T,\omega)$ dependence (Figure 2) may be a characteristic of an increase polarization mobility of sodium cations in the β-phase of $Na_3Fe_2(PO_4)_3$.

Thus, the increase in (ε_i) at frequency (ω_i) with increasing temperature (T) indicates an increase in thermal polarization mobility ($\mu_p(T,\omega)$, K^{-1}):

$$\mu_p(T,\omega_i) = \frac{\varepsilon_2(T,\omega_i) - \varepsilon_1(T,\omega_i)}{T_2 - T_1} = \frac{\Delta\varepsilon(T,\omega_i)}{\Delta T} \quad (5)$$

where ε_1 and ε_2 are the dielectric constants of the sample at frequencies ω_1 and ω_2 of the electric field at the corresponding temperatures T.

Unlike α-$Na_3Fe_2(PO_4)_3$, the structure of the $Na_3FeTi(PO_4)_3$ polycrystal formed during synthesis exhibits the hexagonal R-3c crystal system. Moreover, the value of ε for the β-$Na_3FeTi(PO_4)_3$ sample is significantly higher, whilst $\mu_p(T,\omega)$ (the slope of the $\varepsilon(T,\omega)$ curve) is slightly lower than that of α-$Na_3Fe_2(PO_4)_3$. The higher polarisation of β-$Na_3FeTi(PO_4)_3$ is likely to be due to a higher concentration of sodium cations per unit volume. The decrease in the value of $\mu_p(T,\omega)$ for β-$Na_3FeTi(PO_4)_3$ compared with α-$Na_3Fe_2(PO_4)_3$ can be attributed to the relative reduction in the M(2) voids of the anionic crystal structure between the samples (the unit cell parameters of β-$Na_3FeTi(PO_4)_3$ are smaller than those of α-$Na_3Fe_2(PO_4)_3$.

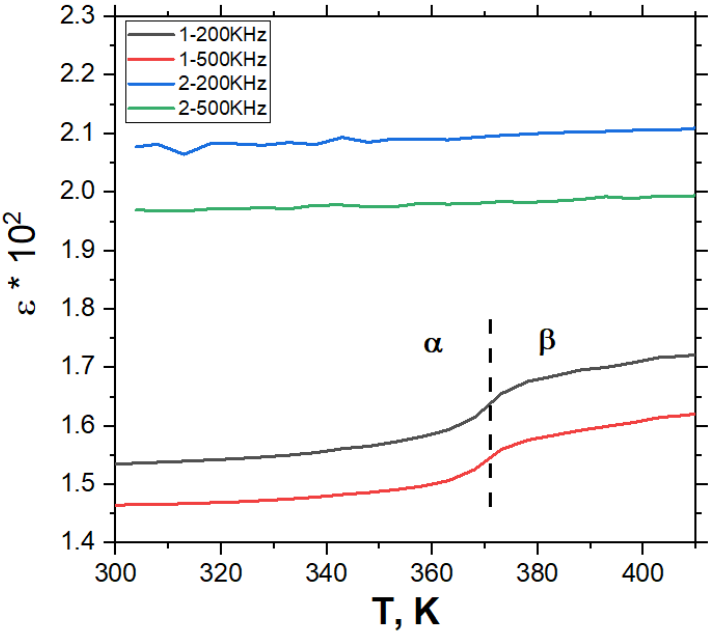

Figure 2. Dependences ($\varepsilon(T,\omega)$) for $Na_3Fe_2(PO_4)_3$ and $Na_3FeTi(PO_4)_3$ polycrystals at frequencies of 200 and 500 kHz.

The results of the studies, together with the data from [12], make it possible to schematically illustrate the distribution of sodium cations in the M(1) and M(2) cavities of the anionic crystal structure of the α- and β-phases of the $Na_3Fe_2(PO_4)_3$ and $Na_3FeTi(PO_4)_3$ samples (Table 3).

Table 3.
A schematic representation of the distribution of sodium cations in the M(1) and M(2) voids of the crystal structures of the α- and β-phases of $Na_3Fe_2(PO_4)_3$ and β-$Na_3FeTi(PO_4)_3$ samples. α-phase: ⇄ – large compensated sodium dipoles of the AFE type; ⇄ – small compensated sodium dipoles of the AFE type; ⊕ – ordered sodium cations; β-phase: ◯ – disordered sodium cations.

Sample compositions	Phases	Voids of the crystal structures			
		M(1)	M(2)		
$Na_3Fe_2(PO_4)_3$	α		⇄	⇄	⊕
	β	◯	◯	◯	⊕
$Na_3FeTi(PO_4)_3$	β	◯	◯	◯	⊕

The ionic conductivities of the crystallites of the $Na_3Fe_2(PO_4)_3$ and $Na_3FeTi(PO_4)_3$ polycrystals were determined by the impedance method. The temperature dependences of the conductivity $\sigma(T)$ of the samples are shown in Figure 3. The conductivity of the $Na_3FeTi(PO_4)_3$ polycrystal is linear in the $\sigma(T)$ dependence, since its structure is formed by the rhombohedral phase.

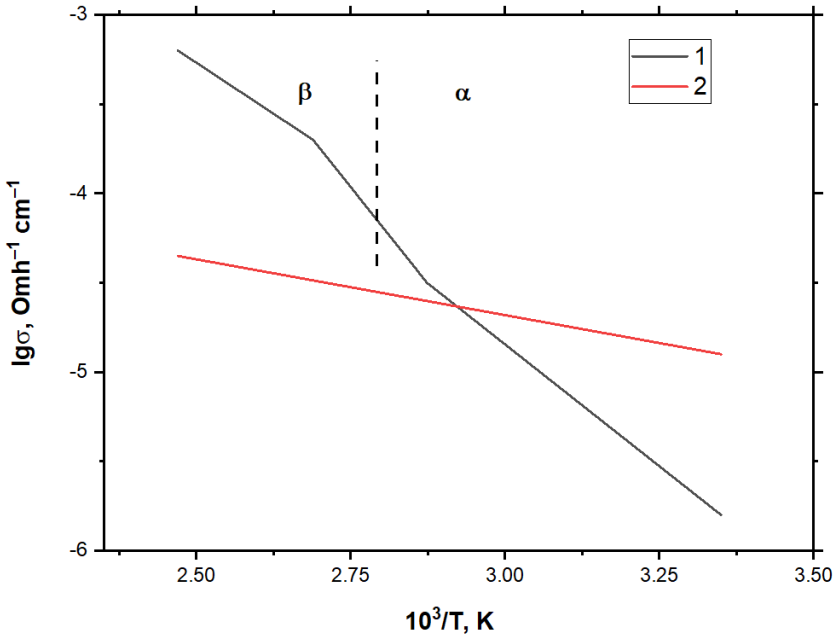

Figure 3. $\sigma(T)$ dependences of polycrystals for $Na_3Fe_2(PO_4)_3$ (1) and β - $Na_3FeTi(PO_4)_3$ (2).

The $\sigma(T)$ dependence in Figure 3 shows that the conductivity values of $Na_3Fe_2(PO_4)_3$ are divided into the low-conductivity α - and high-conductivity β-phases. The conductivity of the $Na_3Fe_2(PO_4)_3$ (1) polycrystal in the α-phase has low σ values and high activation energy (ΔE) values, but in the β-phase its σ increases sharply, and ΔE decreases. In general, the conductive properties of β - $Na_3FeTi(PO_4)_3$ (2) are better than those of α - $Na_3Fe_2(PO_4)_3$, and their $\sigma(T)$ dependences obey the Arrhenius law:

$$\sigma_{\alpha,\beta} = \sigma_{0\alpha,\beta} \exp\left(-\frac{\Delta E_{\alpha,\beta}}{kT}\right), \tag{6}$$

where $\sigma_{0\alpha}$ and $\sigma_{0\beta}$ are pre-exponential factors for α-phases and β-phases; ΔE_α and ΔE_β are the activation energies of conductivity for the α- and β-phases; k is the Boltzmann constant; and T is the absolute temperature.

To quantitatively evaluate the conductive properties, the conductivity parameters of both samples were determined by processing the experimental data and are presented in Table 4.

Table 4.
Conductivity parameters for $Na_3Fe_2(PO_4)_3$ and $Na_3FeTi(PO_4)_3$.

Parameters	Phases	Polycrystal compositions	
		$Na_3Fe_2(PO_4)_3$	$Na_3FeTi(PO_4)_3$
Ionic Conductivity σ, $(Ohm \cdot cm)^{-1}$	α (300 K)	$1.2 \cdot 10^{-6}$	β-phase $2.1 \cdot 10^{-5}$
	β (373 K)	$2.3 \cdot 10^{-4}$	$6.2 \cdot 10^{-5}$
Activation Energy ΔE, eV	α	0.63	β-phase 0.15
	β	0.46	0.15

The established conductive properties of $Na_3Fe_2(PO_4)_3$ and $Na_3FeTi(PO_4)_3$ correlate with the results of studies of their dielectric properties.

Discussion

It should be noted that the conductivity of $Na_3FeTi(PO_4)_3$ polycrystalline at room temperature is higher than that of $Na_3Fe_2(PO_4)_3$ polycrystalline, which is an important advantage for its practical application as a cathode material in NIBs. The ionic conductivity (σ) of both samples can be described by a linear relationship between charge carriers (q), their concentrations (n), and mobility (μ):

$$\sigma = qn\mu \tag{7}$$

According to formula (6), the low conductivity values of the $Na_3Fe_2(PO_4)_3$ polycrystal in the polar α-phase are due to the dipole ordering of sodium cations, i.e., the low concentration and mobility of sodium cations capable of conducting. The conductivity of β-$Na_3Fe_2(PO_4)_3$ increases sharply, and the activation energy decreases, since an increase in the symmetry of the structure leads to dipole disordering and an increase in the mobility of sodium cations.

The higher conductivity of the β-$Na_3FeTi(PO_4)_3$ polycrystal compared with α-$Na_3Fe_2(PO_4)_3$ is likely due to the higher concentration of mobile sodium cations (n) within the cavities of the anionic crystal frameworks, i.e., the cation sublattice of β-$Na_3FeTi(PO_4)_3$ is disordered due to its higher symmetry (R-3c). The low ionic conductivity of α-$Na_3Fe_2(PO_4)_3$ may be attributed to the low concentration of mobile sodium cations, as these are highly dipole-ordered due to the monoclinic distortion of the structure with the C2/m symmetry group. Furthermore, the mobility (μ) of sodium cations in α-$Na_3Fe_2(PO_4)_3$ may be reduced due to a narrowing of the conduction channel, i.e., the 'conduction window' between the M(1) and M(2) cavities of the crystal lattice [12]. The sharp increase in conductivity in β-$Na_3Fe_2(PO_4)_3$ may be attributed to an increase in the concentration of mobile sodium cations due to dipole disorder and an enlargement of the conduction channel, as evidenced by the increase in the crystal structure's symmetry to R3c.

Likely, the higher mobility of sodium cations in the rhombohedral β-phases of the polycrystals $Na_3Fe_2(PO_4)_3$ and $Na_3FeTi(PO_4)_3$ is due to a weakening of the interaction between the anionic and cationic sublattices of the crystal structures.

Conclusion

The melt synthesis method enables the rapid production of β-$Na_3FeTi(PO_4)_3$ polycrystals with 3-Rc hexonanal symmetry, containing unpolarised sodium cations, in contrast to α-$Na_3Fe_2(PO_4)_3$ polycrystals, which form in a monoclinic-distorted symmetry and consist mainly of dipole-ordered sodium-type AFEs.

The advantage of the β-$Na_3FeTi(PO_4)_3$ polycrystal over α-$Na_3Fe_2(PO_4)_3$ is that this material exhibits high ionic conductivity at room temperature, as the cation sublattice is disordered within the voids of the anion crystal framework.

β-$Na_3FeTi(PO_4)_3$ polycrystals may find application as functional materials in those areas of technology where instruments or devices are intended to operate at room temperature.

Acknowledgments

This work was supported by the Science Committee of the Ministry of Science and Higher Education of the Republic of Kazakhstan (Grant No. AP26104305).

References

[1] V. Palomares et al., Energy Environ. Sci. **5** (2012) 5884–5901. [*CrossRef*]
[2] J.-Y. Hwang, S.-T. Myung, Y.-K. Sun, Chem. Soc. Rev. **46** (2017) 3529–3614. [*CrossRef*]
[3] M.M. Arnaiz et al., Mater. Today Proc. **39** (2021) 1118–1131. [*CrossRef*]
[4] Y. Liu et al., ACS Sustainable Chem. Eng. **5** (2017) 1306–1314. [*CrossRef*]
[5] R. Rajagopalan et al., Adv. Mater. **29** (2017) 1605694. [*CrossRef*]
[6] N. Kuganathan, A. Chroneos, Materials **12** (2019) 1348. [*CrossRef*]
[7] A.S. Nogai et al., Ceramics **6** (2023) 2295–2306. [*CrossRef*]
[8] A.S. Nogai et al., J. Compos. Sci. **8** (2024) 354. [*CrossRef*]
[9] A.A. Nogai et al., Eurasian J. Phys. Funct. Mater. **9** (2025) 104–109. [*CrossRef*]
[10] E.A. Asabina et al., Russ. J. Inorg. Chem. **53** (2008) 40–47. [*CrossRef*]
[11] S. Patoux, G. Rousse, J.-B. Leriche, Ch. Masquelier, Chem. Mater. **15** (2003) 2084–2093. [*CrossRef*]
[12] A.S. Nogai et al., Phys. Solid State **62** (2020) 1370–1379. [*CrossRef*]
[13] N. Anantharamulu et al., J. Mater. Sci. **46** (2011) 2821–2837. [*CrossRef*]
[14] K. Trad et al., J. Phys. Chem. C **114** (2010) 10034–10044. [*CrossRef*]